

Supporting Information

New view of graphene oxide biosafety on water environment using an edible fish as a model

Keyi Ma,^{†a} Shupeng Zhang,^{†bc} Baoqing Ye,^a Jianyong Ouyang^c and Gen Hua Yue^{*ade}

^a Molecular Population Genetics and Breeding Group, Temasek Life Sciences Laboratory,

National University of Singapore, Singapore, 117604, Singapore. E-mail: genhua@tll.org.sg;

Tel: +65 68727405

^b School of Chemical Engineering, Nanjing University of Science and Technology, Nanjing,

210094, P. R. China.

^c Department of Materials Science and Engineering, National University of Singapore, 117576,

Singapore.

^d Department of Biological Sciences, National University of Singapore, Singapore, 117543,

Singapore.

^e School of Biological Sciences, Nanyang Technological University, Singapore, 637551,

Singapore.

† These authors contributed equally to this work.

1. Functional structures and physicochemical characterization of graphene oxide (GO)

In our study, graphite oxide was homogeneously dispersed in deionized water to form GO. Its nanostructure and dispersion image in water is shown in Fig. S1. The oxygen-containing functional groups located on the surface and edges of GO increase its dispersibility significantly in water.

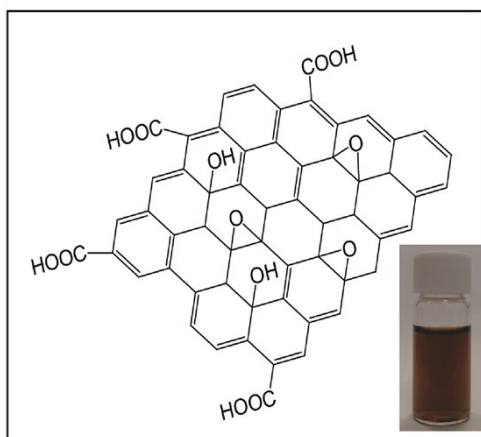


Fig. S1 Structure and dispersion image in water (inset) of GO.

The existence of these hydrophilic groups on GO could be confirmed by FT-IR as shown in Fig. S2a. The oxygen-containing functional groups of GO are revealed by the bands at 3352, 1730 and 1069 cm^{-1} , which are attributed to the OH of COOH groups, C=O stretching of COOH groups and C-O stretching vibrations, respectively. The peak at 1601 cm^{-1} can be attributed to the vibrations of the adsorbed water molecules and also the skeletal vibrations of unoxidized graphite domains.¹ Further evidence for the existence of various functional groups on the graphene surface is observed in the XPS spectrum. Fig. S2b shows the C1s XPS spectra of GO. GO has several different peaks centered at 285.1, 284.4, 286.6, 287.9 and 288.6 eV, corresponding to C-OH (epoxy), graphitic or sp^2 carbon in aromatic rings, C-O-C groups, C=O groups and C(O)-O groups, respectively.

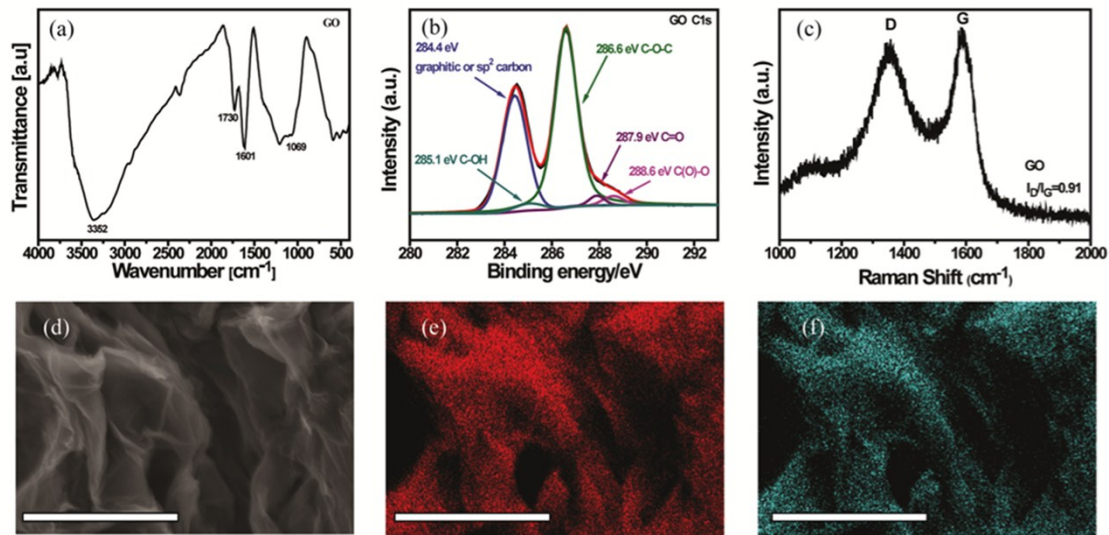


Fig. S2 FT-IR (a), XPS (b), Raman (c), SEM image (d), carbon (e) and oxygen (f) element mapping of GO. The scale bar is 9 μm .

Raman spectroscopy offers an efficacious tool to probe the structural characteristics and properties of graphene-based nanomaterials. Fig. S2c shows the typical Raman spectrum of GO. In the spectrum of GO, the peak at 1580 cm^{-1} (G-band) is due to an E_{2g} mode of graphite and is related to the vibration of sp^2 -bonded carbon atoms in a 2D hexagonal lattice. Owing to the breathing mode of A_{1g} symmetry, the peak at 1357 cm^{-1} (D-band) is associated with vibrations of carbon atoms with dangling bonds from in-plane terminations of disordered graphite. Notably, the ratio of the intensities (I_D/I_G) for GO is 0.91, indicating the formation of some sp^3 carbon by oxygen functionalization with the decrease of sp^2 domains. Altogether, the results of FT-IR, XPS and Raman are consistent.²

Fig. S2d shows typical SEM images of GO nanosheets. The GO is partly aggregated due to the π - π stacking among individual graphene sheets. In order to investigate the distribution of carbon and oxygen in GO, elemental mapping was performed. The distribution of carbon (Fig. S2e), in accordance with that of oxygen (Fig. S2f), actually reflects the morphology of the area shown in Fig. S2d. These results

confirm that the carbon and oxygen atoms are uniformly distributed in the framework of GO.

2. Analysis of gut microbiota in experimental and control fish

After trimming of unassembled reads and low-quality sequences from the two-paired ends, 9,744,685 and 12,608,376 high-quality reads from the four experimental and the four control samples, respectively, were obtained in total, giving an overall average length of 415 base pairs for 16S rRNA V3 and V4 regions. The high-quality reads were further classified by phylum, class and order using the program Mothur with default setting, and the top 20 taxa at class and order levels are shown in Tab. S1.

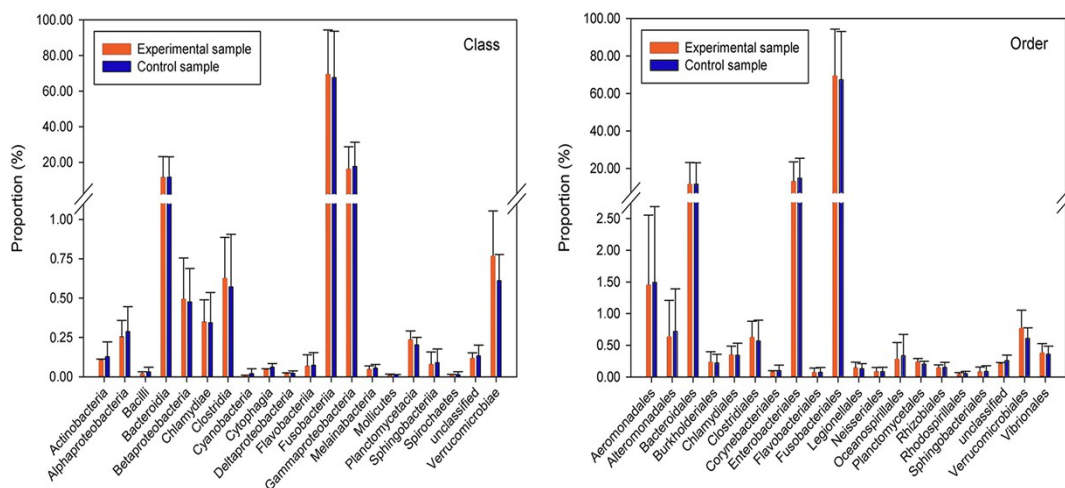


Fig. S3 Comparison, between experimental fish and control fish, of taxonomic composition in tilapia gut microbiota in response to ingestion of GO-adsorbed food. The proportions for the top 20 taxa at class and order levels are presented. The histograms represent the means + standard error (SE) of the data. No difference shown ($P > 0.05$) between the experimental fish and the control fish.

Table. S1 The top 20 taxa at phylum, class, and order levels in tilapia gut microbiota of both experimental fish and control fish. Samples A6, A8, B6 and B10 are from intestines of tilapia fed with GO-absorbed feed; samples A7, A9, B3 and B11 are from fish fed with normal feed.

Phylum	Proportion (%)							
	A6	A8	B6	B10	A7	A9	B3	B11
Acidobacteria	0.006	0.007	0.003	0.002	0.007	0.001	0.003	0.004
Actinobacteria	0.104	0.108	0.118	0.099	0.086	0.129	0.047	0.260
Aquificae	0.002	0.001	0.001	0.000	0.002	0.000	0.001	0.000
Bacteroidetes	20.812	22.997	1.585	1.083	21.075	22.791	2.482	0.973
Chlamydiae	0.514	0.403	0.281	0.190	0.444	0.559	0.229	0.143
Chlorobi	0.003	0.004	0.002	0.002	0.005	0.001	0.008	0.002
Chloroflexi	0.013	0.011	0.001	0.001	0.022	0.013	0.001	0.001
Chrysiogenetes	0.003	0.001	0.000	0.001	0.002	0.001	0.001	0.001
Cyanobacteria	0.104	0.069	0.034	0.026	0.131	0.113	0.034	0.043
Deinococcus-Thermus	0.001	0.003	0.000	0.000	0.002	0.002	0.000	0.000
Firmicutes	0.887	0.880	0.494	0.337	0.763	1.051	0.354	0.279
Fusobacteria	46.514	48.755	89.128	92.682	47.546	42.579	7.208	91.966
Lentisphaerae	0.001	0.003	0.000	0.000	0.002	0.002	0.001	0.000
Planctomycetes	0.233	0.163	0.312	0.240	0.177	0.270	0.171	0.212
Proteobacteria	30.258	25.873	6.850	4.512	29.150	31.847	88.589	5.473
Spirochaetae	0.011	0.016	0.001	0.001	0.041	0.010	0.001	0.001
Synergistetes	0.002	0.003	0.000	0.000	0.005	0.000	0.000	0.000
Tenericutes	0.008	0.021	0.001	0.001	0.015	0.011	0.001	0.001
Thermotogae	0.001	0.001	0.000	0.000	0.002	0.001	0.000	0.000
Verrucomicrobia	0.478	0.639	1.155	0.792	0.462	0.563	0.849	0.576

Class	Proportion (%)							
	A6	A8	B6	B10	A7	A9	B3	B11
Actinobacteria	0.101	0.102	0.117	0.099	0.083	0.121	0.046	0.260
Alphaproteobacteria	0.366	0.318	0.183	0.146	0.354	0.480	0.144	0.171
Bacilli	0.021	0.037	0.008	0.009	0.062	0.049	0.009	0.006
Bacteroidia	20.485	22.618	1.513	1.024	20.646	22.427	2.344	0.921
Betaproteobacteria	0.643	0.783	0.310	0.230	0.670	0.650	0.296	0.284
Chlamydiae	0.514	0.403	0.281	0.190	0.444	0.559	0.229	0.143
Clostridia	0.855	0.832	0.483	0.325	0.685	0.991	0.341	0.269
Cyanobacteria	0.008	0.012	0.001	0.000	0.066	0.013	0.001	0.000
Cytophagia	0.049	0.049	0.047	0.038	0.071	0.050	0.087	0.030
Deltaproteobacteria	0.017	0.029	0.010	0.009	0.044	0.015	0.014	0.009
Flavobacteriia	0.124	0.135	0.004	0.003	0.163	0.119	0.007	0.003
Fusobacteriia	46.514	48.755	89.128	92.682	47.546	42.579	88.104	91.966
Gammaproteobacteria	29.212	24.716	6.240	4.043	28.053	30.677	7.208	4.854
Melainabacteria	0.079	0.043	0.032	0.025	0.056	0.087	0.032	0.043
Mollicutes	0.008	0.021	0.001	0.001	0.015	0.011	0.001	0.001
Planctomycetacia	0.233	0.161	0.305	0.234	0.173	0.268	0.162	0.207
Sphingobacteriia	0.129	0.162	0.009	0.009	0.157	0.171	0.022	0.007
Spirochaetes	0.011	0.016	0.001	0.001	0.041	0.010	0.001	0.001
unclassified	0.080	0.092	0.159	0.129	0.112	0.101	0.080	0.234
Verrucomicrobiae	0.475	0.635	1.154	0.791	0.458	0.559	0.848	0.574

Order	Proportion (%)							
	A6	A8	B6	B10	A7	A9	B3	B11
Aeromonadales	2.651	2.115	0.626	0.403	2.442	2.611	0.543	0.376
Alteromonadales	1.303	0.925	0.173	0.116	1.214	1.385	0.138	0.137
Bacteroidales	20.485	22.618	1.513	1.024	20.646	22.427	2.344	0.921
Burkholderiales	0.303	0.435	0.108	0.077	0.337	0.344	0.112	0.099
Chlamydiales	0.514	0.403	0.281	0.190	0.444	0.559	0.229	0.143
Clostridiales	0.848	0.828	0.482	0.324	0.677	0.984	0.339	0.269
Corynebacteriales	0.061	0.060	0.103	0.090	0.045	0.083	0.038	0.231
Enterobacteriales	23.700	20.287	4.940	3.182	22.859	25.067	7.208	3.889
Flavobacteriales	0.124	0.135	0.004	0.003	0.163	0.119	0.007	0.003
Fusobacteriales	46.514	48.755	89.128	92.682	47.546	42.579	87.007	91.966
Legionellales	0.209	0.232	0.070	0.047	0.181	0.215	0.061	0.068
Neisseriales	0.025	0.019	0.159	0.122	0.025	0.021	0.149	0.140
Oceanospirillales	0.565	0.443	0.054	0.036	0.563	0.683	0.048	0.043
Planctomycetales	0.232	0.160	0.304	0.233	0.169	0.268	0.162	0.207
Rhizobiales	0.194	0.171	0.108	0.086	0.171	0.257	0.079	0.103
Rhodospirillales	0.070	0.063	0.025	0.021	0.087	0.083	0.022	0.026
Sphingobacteriales	0.129	0.162	0.009	0.009	0.157	0.171	0.022	0.007
unclassified	0.204	0.223	0.223	0.176	0.351	0.230	0.148	0.302
Verrucomicrobiales	0.475	0.635	1.154	0.791	0.458	0.559	0.848	0.574
Vibrionales	0.532	0.471	0.297	0.200	0.476	0.461	0.226	0.274

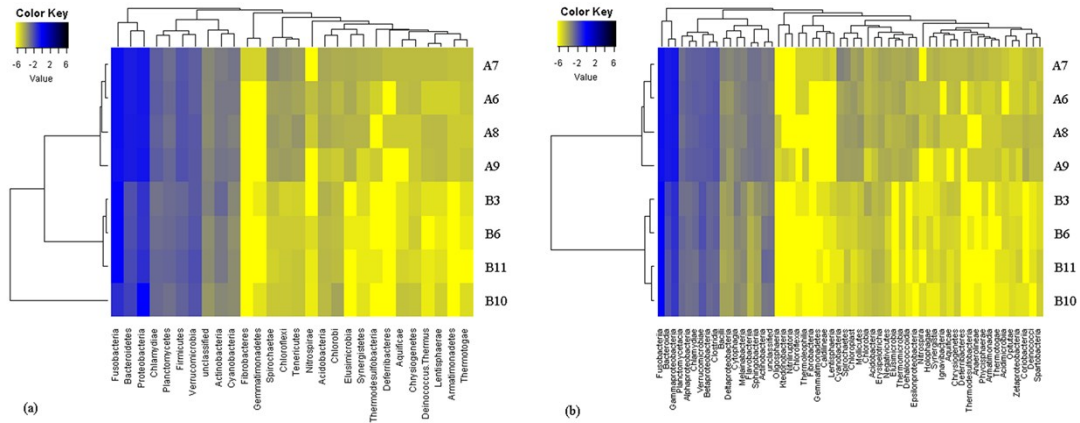


Fig. S4 Heatmap of bacterial distributions in the four experimental fish and the four control fish at phylum and class levels. The bacterial phylogenetic tree was calculated using the neighbor-joining method and the relationship among the eight samples was determined by Bray distance method. The heatmap plot depicts the relative proportion (log-transformed values), of each bacterial phylum (a) or class (b) within each sample by color intensity. The experimental samples are A6, A8, B6 and B10 and the control samples are A7, A9, B3 and B11.

3. Functional analysis of gene expression on tilapia after intake of GO-absorbed feed

A wide range of causes, such as pharmaceuticals and toxins, can affect the oxidative status of fish. The GST and GPX are in response to oxidative stress in organisms including tilapia.³ Metabolism is a set of life-sustaining chemical transformations within an organism, which allows the organism to grow and reproduce, maintain its structure, and respond to its living environment. Among metabolism-related genes, FAS can directly control the synthesis of body fat and is involved in lipid deposition,⁴ and FAD and CPT-1 are essential in fatty acid metabolism.^{5, 6} PDK-2, G6PD, GK and G6 are associated with carbohydrate metabolism.^{6, 7}

4. Materials and methods

4.1 Chemicals and preparation of GO and its characterization

Graphite oxide was synthesized from natural flake graphite using a modified Hummers method.⁸ In a typical procedure, $K_2S_2O_8$ (10 g), P_2O_5 (10 g) and graphite powder (20 g) were put into concentrated H_2SO_4 (30 mL) at 80 °C. The above solution was stirred at 80 °C for 6 h. After cooling to room temperature (22 °C), the solution was diluted with about 2 L of deionized water and allowed to stand overnight. The supernatant was decanted, and the sediment was washed several times with deionized water and centrifuged. The pretreated graphite was dried in air at 25 °C for 12 h. This pretreated graphite powder (20 g) was put into concentrated H_2SO_4 (460 mL) in an ice bath. $KMnO_4$ (60 g) was added gradually with stirring, and the temperature of the solution was kept below 20 °C. After the mixture was stirred at 35 °C for 2 h, 920 mL deionized water was added. The solution was then stirred for another 15 min, and the reaction was then terminated by adding 2800 mL of deionized water and 50 mL of 30% H_2O_2 solution. The mixture was further washed with 5000 mL of 10% HCl solution. The GO thus obtained was re-dispersed in deionized water and then dialyzed for one week to remove residual salts and acids.⁹

The XPS spectra were acquired using an Axis Ultra DLD X-ray photoelectron spectrometer equipped with an Al Ka X-ray source of 1486.6 eV. The resolutions were 1 eV for XPS survey scans and 0.05 eV for XPS fine scans. The binding energies were calibrated with the C 1s XPS band at 284.5 eV. The morphologies of the prepared samples were investigated with a Zeiss Supra 40 field emission scanning electron microscope (SEM).

4.2 Ethics statement

All handling of fish was conducted in accordance with the guidelines on the care and use of animals

for scientific purposes set up by the Institutional Animal Care and Use Committee (IACUC) of the Temasek Life Sciences Laboratory, Singapore. The IACUC has specially approved this study within the project "Breeding of Tilapia" (approval number is TLL (F)-12-004).

4.3 Coating feed surface with GO, fish management and model construction

Five mL of GO water solution with a concentration of 400 $\mu\text{g/mL}$ was mixed uniformly with 30 g of fish pelleted feed (Biomar, Nersac, FR, France), stirred and dried in an oven until the water solvent evaporated. At the beginning of the experiment, some of the feed, both GO-absorbed and normal, was thrown into aquaculture water, immersed for 30 s and pulled out from the water. ("30 s" is the time within which the fish have been observed to finish eating all the feed thrown into the water. Actually, most of the feed could be eaten within 3 ~ 8 seconds.) The immersed feed was then tested to see whether GO could still be absorbed onto the surface of the feed after immersing in water. The normal feed was used as control. After the confirming that GO could indeed be absorbed onto the feed surface, the GO-absorbed and normal feed would be fed to the experimental and control fish groups, respectively, without having to go through the 30 s immersion and subsequent testing any more.

A hybrid tilapia stock from crossing Mozambique tilapia and red tilapia was raised in freshwater in the animal facility and fed twice daily at 10 am and 4 pm. The fish, with average body weight of 20 ± 3.35 g, were divided equally into two groups and raised temporarily in recirculating tanks, each with water volume of 100 L, at a temperature of 26 ± 1 °C for 10 days. Subsequently, the 15 fish in the experimental tank were fed twice daily using ~ 2 mg of GO-absorbed feed. The 15 fish in the control tank were fed with normal feed. The feeding continued for 30 days so as to further analyze the influence of GO on the growth status, diversity and composition of gut microbiota, gene expression, histology and

scanning electron microscope (SEM) assay.

In this study, tilapia and the aquatic water were used as a model for aquatic living things and their environment. An artificial water circulatory system was used to simulate the self-cleaning capacity of the water in nature. Meanwhile, the GO-absorbed feed was used to simulate GO being dispersed into water and ingested by aquatic living things.

4.4 Sample preparation and gut bacterial DNA extraction

Eight fish (four from the experimental group, the other four from the control group) were randomly selected and euthanized using AQUI-S® (NEW ZEALAND LTD, Lower Hutt, New Zealand). Entire intestines were removed from the fish using sterile scissors and tweezers, and the contents were gently squeezed out and harvested. Thereafter, the intestines were split longitudinally and the epithelial intestinal mucosa were scraped with tips and washed using 1× phosphate-buffered saline solution (1× PBS). Subsequently, the contents from the intestines were pooled together with the corresponding epithelial mucosa and the 1× PBS used for washing. Lastly, the mixtures were ground and centrifuged at low speed to isolate food residue, and then filtered with a 100 µm Nylon net filter (Millipore, Billerica, MA, USA). The filtrate was centrifuged at full speed for 30 min. Then the cells were collected for isolation of metagenomic DNA using the QIAamp DNA Stool Mini Kit (Qiagen, Valencia, CA, USA) with slight modification. For each sample, metagenomic DNA was extracted in triplicates to avoid community DNA bias. The integrity of metagenomic DNA was measured by gel electrophoresis, and the purity and concentration were analyzed using Agilent 2100 Bioanalyzer (Agilent, USA). The extracted metagenomic DNA was stored at -20 °C until use.

5. 16S rRNA amplification, sequencing, assembly and bioinformatics analysis

Two regions in the 16S rRNA gene, covering ~180 bp for the V3 and ~240 bp for the V4 regions were selected to construct the community library and for sequencing with Illumina NextSeq 500 sequencing system (Illumina, San Diego, CA, USA). Briefly, the PCR was carried out in quadruple 25 μ L reactions with 5 μ M of each primer, ~10 ng of template metagenomic DNA, 12.5 μ L 2 \times KAPA HiFi Ready Mix, and adding nuclease-free water up to 25 μ L. The amplification program consisted of an initial denaturaton step at 95 $^{\circ}$ C for 3 min, followed by 25 cycles of 95 $^{\circ}$ C for 30 s, 55 $^{\circ}$ C for 30 s and 72 $^{\circ}$ C for 30 s, and finally, 72 $^{\circ}$ C for 5 min. During amplification, negative controls were also performed. Replicated PCR products of the same sample were assembled within a PCR tube and visualized on a 2% agarose gel. Then all the products were cleaned up with QIAquick Gel Extraction Kit (Qiagen, Germany). Further, index PCR was carried out using the Nextera XT Index Kit (Illumina, USA) to attach dualindices and Illumina sequencing adapters. The index PCR was performed in a 50 μ L reaction mix containing a template of 5 μ L purified PCR products mentioned above, 5 μ L Nextera XT Index Primer 1 (N7xx), 5 μ L Nextera XT Index Primer 2 (S5xx), 20 μ L 2 \times KAPA HiFi Ready Mix, and 10 μ L nuclease-free water. The PCR program is similar to the amplicon PCR, except with eight cycles instead. Lastly, we carried out clean up of the PCR products again, library normalization and pooling, library denaturing, and library loading with PhiX control to NextSeq 500 for sequencing. After sequencing, paired-end data were converted from graph signal to FastQ and demultiplexed to the individuals' data using the software bcl2fastq version 2.0. Assembly of the paired-end reads was carried out using PEAR.¹⁰ FastQ was converted to FastA, and the sequences with any ambiguous base were filtered out with the software NGS QC Toolkit.¹¹ The cleaned-up reads were simplified using the 'unique.seqs' command to generate a unique set of sequences, aligned with the 'align.seqs' command, and compared with the bacterial SILVA

database (released version 119). The aligned sequences were further trimmed using the 'filter.seqs' command. Then the 'dist.seqs', 'cluster', 'classify.seqs', and 'classify.otu' commands were performed with the cutoff equal to 0.03 using the software Mothur.¹² The data calculated by the software Mothur was then input into the software R version 3.2.0 to perform the heatmap analysis. Lastly, SPSS 20.0 was used to find out whether there were any significant differences by carrying out one-way ANOVA. Data significance was accepted at the level of $P < 0.05$.

6. Analysis of gene expressions using quantitative real-time PCR (qPCR)

Nine genes (Tab. S2) related to metabolism and response to stress were selected for expression analysis in the gill, intestine, muscle, spleen and liver of fish fed with GO-absorbed and normal feed using qPCR. Gene expression was analyzed as described in Ma et al.¹³ Briefly, a reaction without DNA was used as the negative control. The β -actin of tilapia was used as the reference gene in qPCR assays. For analysis of the gene expression changes, the values of triplicate qPCR were normalized to the β -actin expression, which was calculated by $\Delta\Delta C_t$ method.¹³

Table. S2 Primers used in this study to detect the gene expression in tilapia.

Gene	Primer sequence (5'-3')	Direction
CPT-1 ⁶	GCCGCCTTCTTTGTGACACT	Forward
	TCTAAACTGGCTGCTGGGTCAT	Reverse
PDK-2 ⁶	CCGCGTAGACAATGGTCGTA	Forward
	GAAATGGGCAGGCCATAGC	Reverse
FAD ⁵	CTATGCTGGAGAGGATGCCACGG	Forward
	CAGCAGGATGTGACTGAGGTGGAG	Reverse
FAS ¹⁴	TGAAACTGAAGCCTTGTGTGCC	Forward
	TCCCTGTGAGCGGAGGTGATTA	Reverse
GPX ¹⁵	CCAAGAGAACTGCAAGAACGA	Forward
	CAGGACACGTCATTCCTACAC	Reverse
GST ¹⁵	TAATGGGAGAGGGAAGATGG	Forward
	CTCTGCGATGTAATTCAGGA	Reverse
GK ¹⁶	GCAGCGAGGAAGCCATGAAGA	Forward
	GAGGTCCCTGACGACTTTGTGG	Reverse
G6 ¹⁶	AGCGCGAGCCTGAAGAAGTACT	Forward
	ATGGTCCACAGCAGGTCCACAT	Reverse
G6PD ¹⁶	ACAGGAACTGTCAGCCCACCTT	Forward
	AGCACCATGAGGTTCTGGACCA	Reverse
β -actin ¹⁷	TGACCCAGATCATGTTCGAGAC	Forward
	GTGGTGGTGAAGGAGTAGCC	Reverse

7. Analysis of liver samples using histology and scanning electron microscope (SEM)

Liver tissues of both the experimental and control groups were dissected and fixed in 4% paraformaldehyde or 2.5% glutaraldehyde and post-fixed in 1% osmium tetroxide solution overnight at 4 °C for histological observation or SEM, respectively. For histological observation, the fixed tissues were

washed three times in 1×PBS, and dehydrated in ascending concentration of ethanol, cleaned in Histo-Clear (National Diagnostics, USA) and embedded in paraffin wax. Sections of 4 ~ 6 μm thickness were prepared using a rotary microtome (Leica) and stretched on albumenized slides. The slides were fixed at 37 °C overnight. Then the sections were deparaffinised in Histo-Clear and hydrated in descending concentrations of ethanol, down to distilled water. Further, the slides were stained in haematoxylin for 10 ~ 15 min, differentiated in 1% hydrochloric acid diluted in ethanol and blued in tap water. After washing, the sections were stained in 0.5% eosin solution for 1 min. The dehydrated and cleaned sections were then mounted in Neutral balsam and observed under microscope (Leica). For SEM the tissues were gradually dehydrated in ascending concentrations of acetone, critical point-dried and sputter-coated with gold. Analysis and imaging of the tissues were performed using a Jeol JSM-6360LV scanning electron microscope operated at 30 kV.

Notes and references

- 1 Y. X. Xu, H. Bai, G. W. Lu, C. Li and G. Q. Shi, *J. Am. Chem. Soc.*, 2008, **130**, 5856.
- 2 J. F. Shen, N. Li, M. Shi, Y. Z. Hu and M. X. Ye, *J. Colloid Interface Sci.*, 2010, **348**, 377.
- 3 D. Gutiérrez-Praena, M. Puerto, A. I. Prieto, Á. Jos, S. Pichardo, V. Vasconcelos and A. M. Cameán, *Environ. Toxicol. Chem.*, 2012, **31**, 1548.
- 4 J. Tian, F. Wu, C. G. Yang, M. Jiang, W. Liu and H. Wen, *Fish Physiol. Biochem.*, 2014, **41**, 1.
- 5 S. Tanomman, M. Ketudat-Cairns, A. Jangprai and S. Boonanuntanasarn, *Comp. Biochem. Physiol., Part B: Biochem. Mol. Biol.*, 2013, **166**, 148.
- 6 B. Speers-Roesch, E. Sandblom, G. Y. Lau, A. P. Farrell and J. G. Richards, *Am. J. Physiol.: Regul., Integr. Comp. Physiol.*, 2010, **298**, R104.

- 7 J. Qiang, J. He, H. Yang, H. Wang, M. D. Kpundeh, P. Xu and Z. Zhu, *J. Therm. Biol.*, 2014, **40**, 25.
- 8 W. S. Hummers and R. E. Offeman, *J. Am. Chem. Soc.*, 1958, **80**, 1339.
- 9 W. H. Cai, T. Lai, W. L. Dai and J. S. Ye, *J. Power Sources*, 2014, **255**, 170.
- 10 J. J. Zhang, K. Kobert, T. Flouri and A. Stamatakis, *Bioinformatics*, 2014, **30**, 614.
- 11 R. K. Patel and M. Jain, *PLoS One*, 2012, **7**, e30619.
- 12 P. D. Schloss, S. L. Westcott, T. Ryabin, J. R. Hall, M. Hartmann, E. B. Hollister, R. A. Lesniewski, B. B. Oakley, D. H. Parks and C. J. Robinson, *Appl. Environ. Microbiol.*, 2009, **75**, 7537.
- 13 K. Y. Ma, J. Y. Lin, S. Z. Guo, Y. Chen, J. L. Li and G. F. Qiu, *Gen. Comp. Endocrinol.*, 2013, **185**, 90.
- 14 J. Tian, F. Wu, C. G. Yang, M. Jiang, W. Liu and H. Wen, *Fish Physiol. Biochem.*, 2014, 1.
- 15 D. Gutioliol-Praena, M. Puerto, A. I. Prieto, Á. Jos, S. Pichardo, V. Vasconcelos and A. M. Cameán, *Environ. Toxicol. Chem.*, 2012, **31**, 1548.
- 16 J. Qiang, J. He, H. Yang, H. Wang, M. Kpundeh, P. Xu and Z. Zhu, *J. Therm. Biol.*, 2014, **40**, 25.
- 17 G. H. Fu, Z. Y. Wan, J. H. Xia, F. Liu, X. J. Liu and G. H. Yue, *Fish Shellfish Immunol.*, 2014, **40**, 331.